# Structure Elucidation of Australifungin, a Potent Inhibitor of Sphinganine *N*-Acyltransferase in Sphingolipid Biosynthesis from *Sporormiella australis*

Otto D. Hensens,* Gregory L. Helms, E. Tracy Turner Jones, and Guy H. Harris

*Merck Research Laboratories, P.O. Box 2000, Rahway, New Jersey 07065*

*Received November 14, 1994*[⊗]

The structure elucidation of the novel, potent sphinganine *N*-acyltransferase inhibitor, australifungin (**1**), from *Sporormiella australis* is described. Extensive exchange-broadening phenomena predominantly of the keto–enol type were observed on the NMR time scale which was resolved by derivatization to triacetate (**2**) and tetraacetate (**3**) derivatives. Residual exchange broadening in the acetates was attributed to hindered rotation about the C3–C11 single bond which was frozen out into two conformers at low temperature. The application of 2D NMR techniques to the structure elucidation of the acetate derivatives at ambient and low temperature therefore contributed considerably to the overall structure determination of **1**. The conformation and complete relative stereochemistry followed from a consideration of the Karplus relationship for $^1H-^1H$ vicinal coupling constants and phase-sensitive NOE data. Temperature-dependent NMR experiments suggest an averaged conformational mixture of four to five forms in solution at ambient temperature whereas a predominant conformer **1** is indicated at low temperature with the enolized β-keto aldehyde stabilized through internal H-bonding in the *cis*-orientation. The triacetate **2** and tetraacetate **3**, by contrast, are enolized in the sterically favored *trans* configuration. The β-keto alcohol derivative australifunginol (**6**) is also present.

Ceramide is the precursor of complex sphingolipids and is an intermediate product of sphingolipid catabolism. Recent results suggest that it may function as an intracellular second messenger, analagous to the role of diacylglycerol in glycolipid metabolism.[1] Ceramide is formed by acylation of the long chain bases sphingosine, sphinganine, or 4-hydroxysphinganine by the action of the enzyme sphinganine *N*-acyltransferase (ceramide synthase). Inhibition of ceramide synthase, and subsequent disruption of sphingolipid biosynthesis, is believed to be the mechanism of action of the fumonisin group of mycotoxins.[2] Ingestion of fumonsin-contaminated grain has been associated with equine leukoencephalomacia, porcine pulmonary edema, and higher rates of human esophogeal cancer.[3] We report herein the structure of australifungin (**1**) which was isolated from the coprophilus fungus *Sporormiella australis* (MF5672, ATTC 74157).[4] Australifungin is a potent antifungal agent and the first nonsphingosine-based inhibitor of sphingolipid biosynthesis.

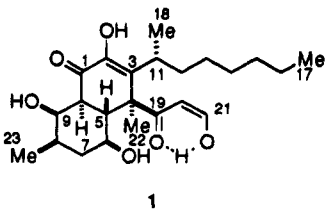


**1**

**Structure Elucidation of Australifungin (1).** The NMR structure elucidation of australifungin (**1**) presented a considerable challenge primarily due to a large number of missing and broadened $^1H$ and $^{13}C$ NMR signals in the spectra at ambient temperature. High-resolution FAB mass spectral data (HR-FABMS) suggested the empirical formula $C_{23}H_{36}O_6$, which formed a tris- and tetrakis(trimethylsilyl) derivative (TMS) on silylation. Only 17 carbons were observed by $^{13}C$ NMR in $CD_2Cl_2$ at ambient temperature, however, which was attributed to exchange-broadening phenomena predominantly associated with keto–enol exchange equilibria. Critical $^1H-^1H$ and $^1H-^{13}C$ connectivities were therefore not observed using the normal repertoire of 2D NMR experiments such as DQF-COSY, TOCSY, HMQC, and HMBC. The compound was, therefore, acetylated in the hope of freezing-out the tautomeric exchange. Triacetate and tetraacetate derivatives were prepared which were more amenable to NMR analysis but nevertheless displayed residual exchange-broadened resonances. For example, two of the 29 carbon resonances for the triacetate $C_{29}H_{42}O_9$ (**2**) recorded at ambient temperature were completely exchange-broadened, whereas all 31 signals of the tetraacetate $C_{31}H_{44}O_{10}$ (**3**) were observed even though 15 were broad and three extremely so (see Table 1). The $^{13}C$ spectrum of **3** comprises 1 × $CH_3$(br s), 1 × $CH_3CH_2$, 2 × $CH_3CH$, 4 × $CH_3CO_2$, 6 × $CH_2$, 1 × C, 4 × CH, 2 × CHO, 2 × CH=, 2 × C=, 2 × $CO_2R$, and 2 × CO. The six oxygens in australifungin therefore comprise two β- and/or α-dicarbonyl systems and 2 × CHOH, whereas the number of unsaturations (six double bonds, 2 × $CO_2R$ and 2 × CO) suggest the presence of two rings. Formation of the triacetate and tetraacetate derivatives from **1** involves acetylation of the two enolic hydroxyls in both cases and one or both secondary alcohols, respectively. From a selection of NMR experiments

[⊗] Abstract published in *Advance ACS Abstracts*, March 1, 1995.

(1) Hannun, Y. A. *J. Biol. Chem.* **1994**, *269*, 3125–3128.
(2) (a) Wang, E.; Norred, W. P.; Bacon, C. W.; Riley, R. T.; Merrill, A. H., Jr. *J. Biol. Chem.* **1991**, *266*, 14486–14490. (b) Merrill, A. H., Jr.; Wang, E.; Gilchrist, D. G.; Riley, R. T. *Adv. Lipid Res.* **1993**, *26*, 215–234.
(3) (a) Nelson, P. E.; Desjardins, A. E.; Plattner, R. D. *Annu. Rev. Phytopathol.* **1993**, *31*, 233–252. (b) Also see the special theme issue concerning fumonisins: *Mycopathologia* **1992**, *117*, 1–124.
(4) Mandala, S. A.; Thornton, R. A.; Frommer, B. R.; Curotto, J. E.; Rozdilsky, W.; Kurtz, M. B.; Giacobbe, R. A.; Bills, G. F.; Cabello, M. A.; Martin, I.; Palaez, F.; Harris, G. H. *J. Antibiot.* **1995**, in press.

0022-3263/95/1960-1772$09.00/0 

**Table 1. $^{13}C$ NMR Data of Australifungin (1), Triacetate (2), and Tetraacetate (3) Derivatives in $CD_2Cl_2$ at Different Temperatures (125 MHz)[a]**

| | 1 | | | | | |
|---|---|---|---|---|---|---|
| carbon | −50 °C[b] | 25 °C[c] | **2** 25 °C[c] | 2 (−25 °C)[d] major/minor | **3** 25 °C[c] | **3** (−25 °C)[e] major/minor |
| 1 | 193.6 | 194.1 | *f* | 189.8/191.0 | 187.3 | 187.17/187.14 |
| 2 | 139.6 | *f* | 144.5* | 143.9/143.5 | 144.6* | 143.9/143.5 |
| 3 | 144.5 | 145.0 | *f* | 155.87/154.8 | 155.5* | 155.3/154.3 |
| 4 | 53.2 | *f* | 56.4 | 56.05/56.23 | 56.4* | 55.8/56.2 |
| 5 | 43.7 | 44.8 | 40.0* | 39.1/39.8 | 41.1* | 40.4/40.8 |
| 6 | 70.0 | 71.0 | 71.5* | 70.85/71.1 | 70.8* | 70.1/70.5 |
| 7 | 33.7 | 35.7 | 32.8 | 32.3/32.1 | 35.2 | 33.6/33.1 |
| 8 | 33.3 | 34.2 | 33.6 | 33.2/32.8 | 33.3 | 32.66/32.68 |
| 9 | 67.3 | 68.0 | 67.7* | 67.3/66.8 | 69.7* | 69.2/68.1 |
| 10 | 47.4 | 48.2 | 49.4 | 48.78/48.63 | 47.9* | 47.3/46.8 |
| 11 | 34.7 | *f* | 36.2* | 35.9/35.4 | 36.5* | 36.1/35.6 |
| 12 | 36.2 | 37.2 | 35.0 | 34.4/34.3 | 34.4* | 34.6/34.4 |
| 13 | 27.8 | 28.4 | 28.5* | 28.2/27.9 | 28.6* | 28.2/27.9 |
| 14 | 29.0 | 29.4 | 29.3 | 28.98/28.92 | 29.4 | 29.1/29.0 |
| 15 | 31.8 | 32.2 | 32.0 | 31.6/31.6 | 32.0 | 31.6/31.6 |
| 16 | 22.7 | 23.0 | 22.9 | 22.71/22.68 | 22.9 | 22.70/22.73 |
| 17 | 14.0 | 14.2 | 14.2 | 14.02/14.06 | 14.1 | 14.02/14.06 |
| 18 | 17.4 | 17.7 | 19.2* | 18.9/18.5 | 19.3* | 18.9/18.6 |
| 19 | 207.6 | *f* | 198.2 | 198.08/198.03 | 198.0 | 197.83/197.78 |
| 20 | 101.6 | 102.2 | 110.7 | 109.89/110.08 | 110.5 | 109.6/109.8 |
| 21 | 166.4 | *f* | 149.0 | 148.43/148.50 | 149.2 | 148.66/148.64 |
| 22 | 13.0 | *f* | 14.1* | 13.3/14.2 | 13.8* | 13.4/14.3 |
| 23 | 16.6 | 17.3 | 17.6 | 17.34/17.38 | 17.4 | 17.05/17.16 |
| 24 | | | 168.7* | 168.9/168.4 | 168.6* | 168.4/168.3 |
| 25 | | | 20.7 | 20.7/20.7 | 20.8 | 20.69/20.69 |
| 26 | | | 170.2 | 170.14/170.11 | 170.1 | 170.2/169.93 |
| 27 | | | 20.4 | 20.3/20.3 | 20.3 | 20.22/20.26 |
| 28 | | | | | 170.2* | 169.94/169.86 |
| 29 | | | | | 20.84* | 20.66/20.66 |
| 30 | | | 167.4 | 167.16/167.22 | 167.4 | 167.15/167.13 |
| 31 | | | 20.8 | 20.7/20.7 | 20.8 | 20.71/20.9 |

[a] Significantly to extremely exchange-broadened resonances are marked with an asterisk. [b] Predominant component of equilibrium mixture containing four to five components. [c] Conformationally averaged species. [d] Conformer ratio ~7:5. [e] Conformer ratio ~3:1. [f] Completely exchange-broadened signals.

**Table 2. $^1H$ NMR Data of Australifungin Triacetate (2) and Tetraacetate (3) Derivatives in $CD_2Cl_2$ at −25 °C (500 MHz)[a]**

| | 2[b] | | 3[c] |
|---|---|---|---|
| position | major | minor | major |
| 5 | 2.97 (dd, 10.8, 13.7) | 2.92 (dd, 10.7, 13.7) | 2.93 (dd, 10.9, 13.5) |
| 6 | 4.73 (dt, 4.2, 10.8) | 4.76 (dt, 4.3, 10.9) | 4.77 (dt, 4.6, 10.9) |
| 7β | ~1.43 (dt, ~ 11) | ~1.43 (dt, ~11) | ~1.33 (m) |
| 7α | ~1.58 (m) | ~1.58 (m) | ~1.66 (m) |
| 8 | ~1.58 (m) | ~1.58 (m) | ~1.76 (m) |
| 9 | 4.31 (br s) | 4.25 (br s) | 5.63 (br s) |
| 10 | 2.29 (dd, 2.2, 13.7) | 2.45 (dd, 2.1, 13.9) | 2.41 (dd, 2.5, 13.6) |
| 11 | ~1.58 (m) | ~1.64 (m) | ~1.57 (m) |
| 12 | ~1.25 (m) | ~1.25 (m) | ~1.26 (m) |
| 13a | ~0.87 (m) | ~0.87 (m) | ~0.84 (m) |
| 13b | ~1.25 (m) | ~1.25 (m) | ~1.26 (m) |
| 14 | ~1.04 (m) | ~1.04 (m) | ~1.03 (m) |
| 15 | ~1.04 (m) | ~1.04 (m) | ~1.03 (m) |
| 16 | ~1.13 (m) | ~1.13 (m) | ~1.14 (m) |
| 17 | 0.76 (t, 7) | 0.77 (t, 7) | 0.76 (t, 7.2) |
| 18 | 1.07 (d, 6.7) | 0.90 (d, 6.4) | 1.06 (d, 6.7) |
| 20 | 6.34 (d, 12) | 6.31 (d, 12) | 6.32 (d, 12.2) |
| 21 | 8.26 (d, 12) | 8.26 (d, 12) | 8.31 (d, 12.2) |
| 22 | 1.16 (s) | 1.21 (s) | 1.16 (s) |
| 23 | 0.94 (d, 6.4) | 0.93 (d, 6.4) | 0.81 (d, 6.9) |
| 25 | 2.20 (s) | 2.17 (s) | 2.18 (s) |
| 27 | 1.782 (s) | 1.777 (s) | 1.79 (s) |
| 29 | | | 1.96 (s) |
| 31 | 2.15 (s) | 2.15 (s) | 2.17 (s) |

[a] Coupling constants are in Hz in parentheses. Relative populations of two conformers in slow exchange for [b] **2** ~7:5 and [c] **3** ~3:1 (minor not shown).

(DQF-COSY, TOCSY, DEPT, HMQC, HMBC, and HMQC-TOCSY) performed on the natural product and the triacetate derivative **2** at ambient temperature, the partial structures **A**–**C** were constructed as shown in Figure 1. Fragments **B** and **C** followed primarily from consideration of the DQF-COSY and HMBC data whereas

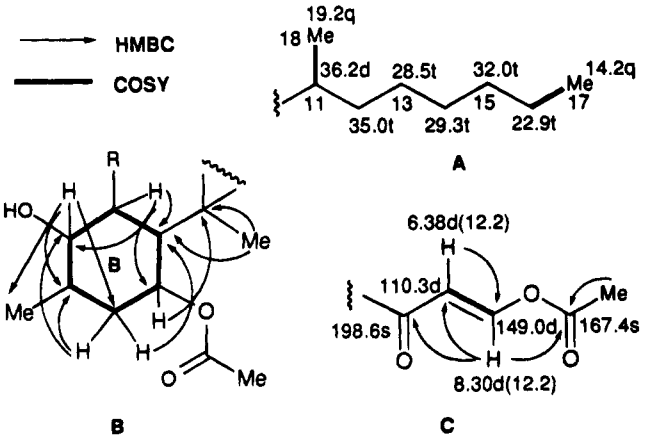


**Figure 1.** Partial structures of australifungin triacetate (**2**).

the 2-methylheptane fragment **A** required consideration of many pieces of information, mainly from a HMQC-TOCSY experiment on the triacetate **2**. For example, H11 showed correlations to C11, C12, C13 (weak), and C18 and the 17-Me triplet to C13 (weak), C14, C15, C16, and C17. The remaining functionalities comprised a tetrasubstituted double bond (C2–C3), a carbonyl group, and one and two acetate units for the triacetate **2** and tetraacetate **3**, respectively. The hydroxyl group at C9 in fragment **B** (Figure 1) is acetylated in the tetraacetate (**3**). Even though the extent of exchange-broadening increases with the frequency difference between the two species in equilibrium and is, therefore, less problematic at 300 than at 500 MHz, acquisition of data at the higher field strength was essential to attain optimal resolution and chemical shift dispersion. However, completion of

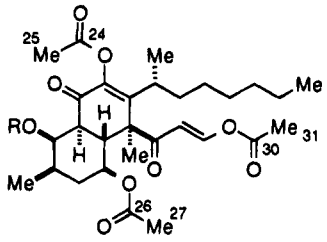

2 R = H

3 R = $^{28}_{}COMe^{29}$

the structure was not possible using solely the data acquired at ambient temperature.

Despite considerable resonance overlap in the upfield region of $^1H$ NMR spectra, determination of the structure was subsequently resolved at low temperature (−25 °C) on the triacetate **2** and tetraacetate **3** derivatives in $CD_2Cl_2$. Sharp solution spectra were obtained showing conformer populations in the proportion of 7:5 and 3:1 for **2** and **3**, respectively. The long-range $^1H-^{13}C$ correlation HMBC data of the triacetate allowed the assembly of partial fragments **A**–**C** into the final structure **2** but not without encountering some initial difficulties. In particular, assignment of the C2 and C3 quaternary carbons at 143.9 and 155.9 ppm (major component) was troublesome as the oxygenated carbon C2 was expected to be downfield of C3. The β-acetoxyvinyl ketone structures **4** and **5** were therefore also considered. The

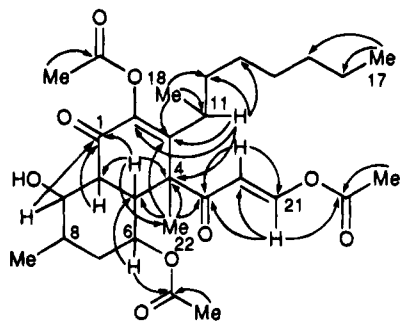

2

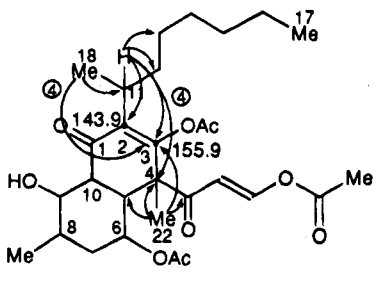

4

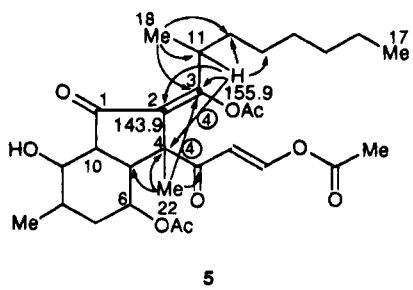

5

absence of the expected 18-Me → C2 correlation in **4** and

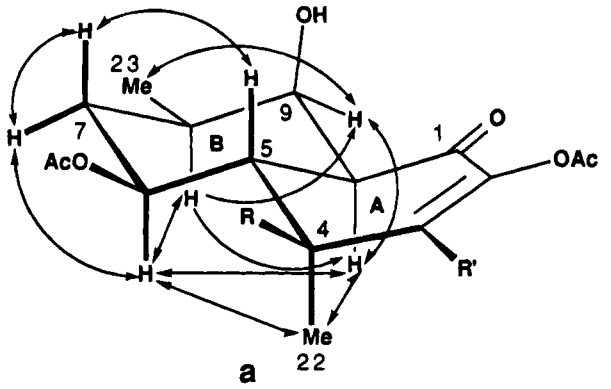

a

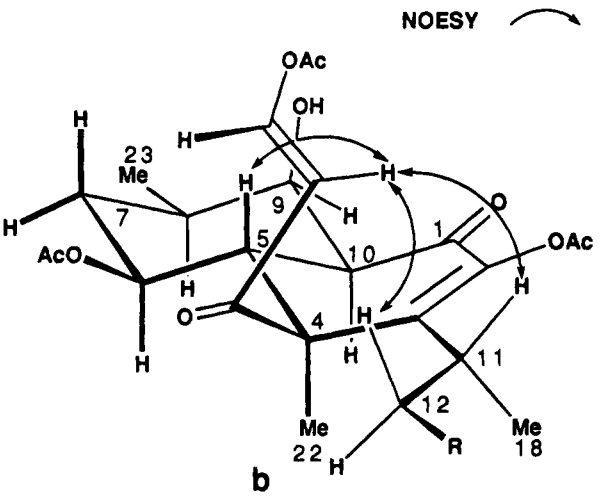

b

**Figure 2.** Conformation and relative stereochemistry of australifungin triacetate (**2**) from NOESY and $^3J_{vic}$ data.

22-Me → C2 bond correlation in **5**, as well as the manifestation of several unlikely four-bond long-range $^1H-^{13}C$ correlations of both structures, are inconsistent with such proposals. In these two examples, assignment of the double bond carbons as indicated (C3 downfield of C2) can be made with a fair degree of certainty as polarization effects of the carbonyl and acetate substituents are expected to reinforce one another as observed in the β-keto aldehyde enol acetate side chain (see Table 1). Even if the assignments were reversed, two 4-bond correlations are evident in both cases. Structure **2**, on the other hand, was constructed utilizing only two- or three-bond correlations where C3 is downfield of C2. Polarization of the C2–C3 double bond in opposite directions by the carbonyl and acetate substituents accounts for the apparently anomalous chemical shifts which are even more marked in the natural product itself (C2 at 139.6 and C3 at 144.5 ppm, Table 1), in accord with the greater electron-donating ability of the enolic OH group. Similar HMBC results confirm these conclusions for the tetraacetate derivative **3**.

**Relative Stereochemistry of Australifungin (1).** The relative stereochemistry was deduced from vicinal $^1H-^1H$ coupling constants ($^3J_{vic}$) and NOEs from phase-sensitive NOESY experiments performed on the triacetate **2** in $CD_2Cl_2$ at −25 °C and corroborated with **3** (Figure 2). The $^3J_{vic}$ values for the major conformer unequivocally define the axial configurations of protons at C10, C5, C6, and C7 (δ ~1.43) as well as an equatorial proton at C7 (δ ~1.58) supporting a normal chair conformation for ring B ($^3J_{10,5} = 13.7$, $^3J_{5,6} = {}^3J_{6,7\beta} = 10.8$, $^3J_{6,7\alpha} = 4.2$ Hz). Approaching the configuration at C9

from H10 (dd $J$ = 2.2, 13.7 Hz) suggests an equatorial orientation for H9 ($^3J_{9,10}$ = 2.2 Hz). The broadened singlet for H9 at $\delta$ 4.31 suggests a small coupling (<0.5 Hz) between H9 and H8 whose configuration may therefore be axial or equatorial. The overlapping H7$\beta$ doublet of triplet multiplets for the two conformers are characterized by three large couplings of the order of 11 Hz, which therefore unequivocally establish the axial configuration of H8. The almost zero *gauche* coupling between H8 and H9 compared with the appreciable coupling $^3J_{6,7\alpha}$ of 4.2 Hz is consistent with the antiperiplanar relationship between H8 and the axial hydroxyl group at C9.[5] These findings are supported in particular by the NOEs observed between the axial protons at C6, C8, and C10 (Figure 2a). The configuration at C4 readily followed from the strong NOEs between the C4-$CH_3$ group and the 1,3-diaxially disposed protons at C6 and C10 assuming a flattened half-chair conformation for ring A, thus confirming the *trans* ring junction. Preferential acetylation of the enol OH groups and the equatorial C6-OH in **2** is consistent with the axial OH configuration at C9.

Deciphering the configuration at C11 in **2** at −25 °C proved more elusive from the NOE data because of considerable resonance overlap in the upfield $^1$H NMR region, exacerbated by the presence of two forms. However, medium to strong NOEs were observed between H20 of the $\beta$-keto aldehyde and H5, H11 and a proton at $\delta$ ~1.25. It should be noted that both protons at C12 and one at C13 are degenerate near $\delta$ 1.25 but that no NOE was observed between H20 and the 18-methyl group. The predominant conformation as depicted in Figure 2b satisfactorily accounts for these findings with the understanding that there is some freedom of rotation of the $\beta$-keto aldehyde moiety about the C4−C19 bond.

$^1$H and $^{13}$C NMR data of the natural product **1** at −25 to −50 °C in $CD_2Cl_2$ indicated multiple equilibria involving four to five different conformers but characterized by one major species at the lowest temperature. This form has the enolized $\beta$-keto aldehyde stabilized through internal H-bonding in the *cis*-orientation as indicated by the 5.7 Hz coupling between H20 and H21. The triacetate and tetraacetate, by contrast, are enolized in the sterically favored *trans* configuration ($^3J_{vic}$ = 12 Hz). That the magnetic field-dependent exchange phenomenon persisted in the two acetate derivatives was quite unexpected, however. The effects of keto−enol exchange equilibria most likely dominates the exchange-broadening phenomena observed in the natural product but can be excluded in the two acetate derivatives. This would account for the complete disappearance of the signals for C2, C4, C11, C19, C21, and C22 in the $^{13}$C spectrum of **1** at ambient temperature. Conformational flipping of ring B can be ruled out on the basis that the observed $^3J_{vic}$ values as well as NOEs are very similar for both major and minor conformers in **2** and **3**. The same appears to hold true for ring A as it is inconceivable that slightly different puckering of ring A from a favored flattened half-chair conformation (see Figure 2) could be frozen out at only −25 °C. This would directly affect the nonbonded interaction between H10 and the C4-$CH_3$ whereas the respective NOEs between them in both conformations are equally prominent. It is more likely that restricted rotation about the C3−C11 bond is responsible for the specific broadening of many of the $^{13}$C resonances noted in Table 1, as a result of a buttressing effect involving the C3 side chain with the methyl and $\beta$-keto aldehyde substituents at C4 and the acetate group at C2. In particular, the resonances for C1, C3, and C22 flanking the C3 side chain are almost completely exchange-broadened. Moreover, the largest $^1$H chemical shift difference for the two conformers is observed for the methyl group at C11 (0.17 ppm) although the significant degree of $^1$H overlap did not allow details of the minor conformation to be elucidated. The buttressing effect appears to be influenced by acetylation at the C9-OH group as the major conformer is now appreciably more stable (3:1 in **3** compared to 7:5 in **2** at −25 °C) which may also be reflected in some broader resonances of ring B and the two involved acetate groups at ambient temperature (see Table 1).

(5) Booth, H. *Tetrahedron Lett.* **1965**, 411.

**Table 3. $^1$H and $^{13}$C NMR Data of Australifunginol (6) in $CD_2Cl_2$**

| carbon | $^{13}$C $\delta^a$ −42 °C | $^{13}$C $\delta^a$ 20 °C | $^1$H $\delta$, mult $J$ in Hz$^b$ 25 °C |
|---|---|---|---|
| 1 | 192.5 | 193.7 | |
| 2 | 139.1 | *c* | |
| 3 | 145.1 | 145.4 | |
| 4 | 55.5 | 55.8* | |
| 5 | 39.8 | 41.4* | 2.86 (dd, 10.5, 13.4) |
| 6 | 69.7 | 70.8 | 3.61 (dt, 4.2, 10.6) |
| 7 | 36.9 | 37.3 | ~1.65 (m) |
| | | | ~1.46 (m) |
| 8 | 33.7 | 34.3 | ~1.62 (m) |
| 9 | 68.7 | 68.4 | 4.40 (br s) |
| 10 | 47.4 | 48.1 | 2.28 (dd, 2.3, 13.6) |
| 11 | 35.5 | 36.1 | ~1.66 (m) |
| 12 | 34.1 | 34.3* | ~1.30 (m) |
| 13 | 28.7 | 28.8 | ~1.25 (m) |
| 14 | 29.5 | 29.7 | ~1.25 (m) |
| 15 | 31.8 | 32.2 | ~1.25 (m) |
| 16 | 22.8 | 23.0 | ~1.25 (m) |
| 17 | 14.0 | 14.2 | 0.87 (t, 6.9) |
| 18 | 17.0 | 17.5 | 1.16 (d, 6.6) |
| 19 | 212.1 | *c* | |
| 20 | 41.4 | *c* | ~1.94 (m) |
| 21 | 60.1 | 59.5 | 3.95 (brm) |
| | | | 3.80 (ddd,3.7, 5.1, 9.0) |
| 22 | 14.0 | 14.7 | 1.36 (v br s) |
| 23 | 17.5 | 17.7 | 1.03 (d, 6.6) |

[a] Significantly to extremely exchange-broadened resonances are marked with an asterisk at 75 MHz. [b] At 400 MHz. [c] Completely exchange-broadened signals.

**Structure Elucidation of Australifunginol (6).** High-resolution electron-impact mass spectral analysis (HR-EIMS) suggested the empirical formula $C_{23}H_{38}O_6$ corresponding to a dihydro derivative of australifungin. Only 20 carbons were observed by $^{13}$C NMR in $CD_2Cl_2$ at ambient temperature (Table 3), but all 23 were clearly in evidence at lower temperature (−42 °C) at 75 MHz. The conspicuous presence of a $-CH_2CH_2OH$ moiety in the molecule and the otherwise similarity to **1** and its acetates by NMR suggested structure **6** having the $\beta$-keto

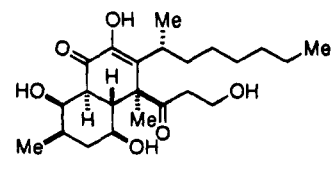


**6**

alcohol instead of the $\beta$-keto aldehyde moiety at C4. The assignments in Table 3 were similarly obtained as for **1** and its acetates. Confirmation of the relationship between **1** and **6** was obtained by reduction of the aldehyde in **1** with sodium cyanoborohydride which gave a product indistinguishable from **6** by HPLC, TLC, and $^1$H NMR.

Australifungin (**1**) is related to stemphyloxin I[6] and the betaenone family of metabolites,[7] in particular betaenone C, which shares the β-keto aldehyde side chain in common with **1**. Betaenone B is the β-keto alcohol derivative of betaenone C, analogous to the co-occurrence of **1** with **6**. Australifungin is a potent antifungal agent versus a panel of clinically relevant *Aspergillus*, *Candida*, and *Cryptococcus* strains with MIC's in the range of <0.015−1.0 μg/mL. It inhibited ceramide synthase *in vitro* with an $IC_{50}$ less than or equivalent to that of fumonisin B1, depending upon the enzyme source. Australifunginol was considerably less active in both assays.[4]

## Experimental Section

**General Methods.** Optical rotations were measured on a Perkin-Elmer Model 241 polarimeter. Infrared spectra were recorded on a Perkin-Elmer Model 1750 Fourier transform spectrometer by multiple internal reflectance as a thin film on ZnSe. Ultraviolet spectra were recorded on a Beckman Model DU70 spectrophotometer.

Mass spectral data were acquired on Finnigan-MAT Models MAT212 and TSQ70B mass spectrometers. MAT212 spectra were obtained in the electron impact (EIMS) mode at 90 eV. Exact mass measurements were performed at high resolution (HR-EIMS) using perfluorokerosene (PFK) as an internal standard. TSQ70B spectra were acquired in the EI mode at 70 eV or by negative-ion fast atom bombardment (FAB-MS) employing ethanolamine as the matrix. Trimethylsilyl derivatives were prepared using a 1:1 mixture of bis(trimethylsilyl)-trifluoroacetamide (BSTFA) and pyridine at 50 °C.

$^1H$ and $^{13}C$ NMR spectra of australifungin (**1**), its triacetate (**2**), and tetraacetate (**3**) were recorded in $CD_2Cl_2$ on a Varian Unity 500 NMR spectrometer at 25 °C and low temperature (see Tables 1 and 2). Due to exchange-broadening processes at ambient room temperature, six $^{13}C$ resonances in **1** were not observed. Two were missing in the triacetate (C1 and C3) under lower S/N conditions than for the tetraacetate where all were observed (but barely for C1, C2, and C22) with appreciable broadening exhibited by some other resonances (indicated in Table 1 by an asterisk). The extent of the broadening was clearly field-dependent and less at lower field (75 MHz) as expected. At −45 °C, australifungin displayed multiple equilibria (from four to five conformers) including one predominant conformer (Table 1). The solution spectra of the triacetate and tetraacetate at −25 °C showed conformer populations in the ratio of *ca.* 7:5 and 3:1, respectively. $^1H$ NMR spectra of australifunginol (**6**) were recorded in $CD_2Cl_2$ on a Varian Unity 400 spectrometer at 25 °C whereas $^{13}C$ NMR spectra were recorded in $CD_2Cl_2$ on a Varian XL-300 spectrometer at ambient temperature and −42 °C. Chemical shifts are given in ppm relative to tetramethylsilane (TMS) using the solvent peak at δ 5.32 ($^1H$) and 53.8 ppm ($^{13}C$) as internal standard. HMBC experiments were optimized for 4 and 7.2 Hz. A mixing and repetition time of 0.5 and 2.5 s, respectively, were used in the phase-sensitive NOESY experiments.

**Australifungin (1):** FAB-MS *m/z* 408.2515 ($M^+$ calcd for $C_{23}H_{36}O_6$ 408.2512), 390.2399 ($M^+ - H_2O$ calcd for $C_{23}H_{34}O_5$ 390.2406), 366.2395 (calcd for $C_{21}H_{34}O_5$ 366.2406), 338.2455 (base peak; calcd for $C_{20}H_{34}O_4$ 338.2457), 320.2334 (calcd for $C_{20}H_{32}O_3$ 320.2351); IR 2929, 2797, 1723 (C=O), 1666 (C=O), 1630 (C=O), 1460, 1398, 1176, 1037 $cm^{-1}$; UV (MeOH) $\lambda_{max}$ 275 nm (ε 13,100), (MeOH + 20 μL of 1 N NaOH) $\lambda_{max}$ 207, 287 (ε 17 300), 306 nm (ε 19 100), (MeOH + 20 μL of 1 N HCl) $\lambda_{max}$ 276 nm (ε 17 300); $[\alpha]^{20}_D$ (MeOH) +98° (*c* 0.59); $^1H$ NMR ($CD_2Cl_2$; −40 °C) δ 0.81 (3H, t, *J* = 7 Hz, 17-$H_3$), 0.97 (3H, d, *J* = 6.5 Hz, 23-$H_3$), 1.07 (3H, d, *J* = 6.7 Hz, 18-$H_3$), 1.47 (3H, s, 22-$H_3$), 2.61 (1H, dd, *J* = 10.1, 13.5 Hz, H5), 3.62 (1H, dd, *J* = 4.5, 10.8 Hz, H6), 4.34 (1H, br s, H9), 5.74 (1H, d, *J* = 5.7 Hz, H20), 7.29 (1H, dd, *J* = 5.6, 11.3 Hz, H21), 9.47 (1H, br d, *J* = 4.3 Hz, OH); $^{13}C$ NMR ($CD_2Cl_2$) see Table 1.

**Acetylation of Australifungin.** Australifungin (20.4 mg) was dissolved in 0.5 mL of pyridine, 0.5 mL of acetic anhydride added, and the mixture stirred at room temperature for 3.75 h. The reaction mixture was then concentrated to dryness *in vacuo*. The residue was dissolved in acetonitrile (5 mL) and the solution concentrated *in vacuo*. The crude reaction mixture was dissolved in 1 mL of acetonitrile and the two acetates purified by preparative HPLC (Whatman Partisil 10 ODS 3, 22 mm × 25 cm, mobile phase of 0.1% $H_3PO_4$ in 60% acetonitrile/40% $H_2O$ eluted at 20 mL/min at room temperature, detection at 275 nm, 8 mL fractions were collected.) Fractions 26−29 contained the triacetate and were pooled and extracted with 32 mL of $CH_2Cl_2$, and the $CH_2Cl_2$ layer was removed, dried over anhydrous $Na_2SO_4$, and concentrated to dryness *in vacuo* to yield 8 mg of australifungin triacetate. Fractions 33−36 were treated similarly to yield 11 mg of australifungin tetraacetate.

**Australifungin triacetate (2):** FAB-MS *m/z* 534.2832 ($M^+$ calcd for $C_{29}H_{42}O_9$ 534.2829); $^1H$ NMR ($CD_2Cl_2$) see Table 2; $^{13}C$ NMR ($CD_2Cl_2$) see Table 1.

**Australifungin tetraacetate (3):** FAB-MS *m/z* 576.2946 ($M^+$ calcd for $C_{31}H_{44}O_{10}$ 576.2935); $^1H$ NMR ($CD_2Cl_2$) see Table 2; $^{13}C$ NMR ($CD_2Cl_2$) see Table 1.

**Australifunginol (6):** HR-EIMS *m/z* 410.2613 ($M^+$ calcd for $C_{23}H_{38}O_6$ 410.2668); IR 2958, 2932, 1698, 1666, 1635, 1397, 1041 $cm^{-1}$; UV (MeOH) $\lambda_{max}$ 275 nm (ε 11 600); $[\alpha]^{20}_D$ (MeOH) +98° (*c* 0.99); $^1H$ and $^{13}C$ NMR ($CD_2Cl_2$) see Table 3.

**Reduction of Australifungin.** Australifungin (5.1 mg, 12.5 μmol) was dissolved in anhydrous THF (0.080 mL) to which was added 0.112 mL (12.5 μmol) of a 7.35 mg/mL solution of $NaBH_3CN$ in THF. After 2 h at rt the reaction mixture was diluted to 1 mL with 0.02 N HCl and extracted with EtOAc, and the EtOAc layer was removed, washed, dried over anhydrous $Na_2SO_4$, and concentrated to dryness under $N_2$. The product was identical to australifunginol by HPLC, TLC, and $^1H$ NMR.

JO941917H

(6) Barash, I.; Manulis, S.; Kashman, Y.; Springer, J. P.; Clardy, J.; Strobel, G. A. *Science* **1983**, *220*, 1065.

(7) (a) Ichihara, A.; Oikawa, H.; Hayashi, K.; Sakamura, S.; Furusaki, A.; Matsunoto, T. *J. Am. Chem. Soc.* **1983**, *105*, 2907. (b) Ichihara, A.; Oikawa, H.; Hashimoto, M.; Sakamura, S.; Haraguchi, T.; Nagano, H. *Agric. Biol. Chem.* **1983**, *47*, 2965. (c) Oikawa, H.; Ichihara, A.; Sakamura, S. *Agric. Biol. Chem.* **1984**, *48*, 2603.